Lu2O3-based storage phosphors. An (in)harmonious family

Kulesza, Dagmara; Bolek, Paulina; Bos, Adrie; Zych, Eugeniusz

DOI
10.1016/j.ccr.2016.05.006

Publication date
2016

Document Version
Accepted author manuscript

Published in
Coordination Chemistry Reviews

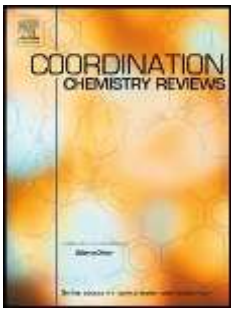

Title: Lu_2O_3-Based Storage Phosphors. An (In)harmonious Family

Author: Dagmara Kulesza, Paulina Bolek, Adrie J.J. Bos, Eugeniusz Zych

PII: S0010-8545(15)30120-X
DOI: http://dx.doi.org/doi: 10.1016/j.ccr.2016.05.006
Reference: CCR 112256

To appear in: *Coordination Chemistry Reviews*

Received date: 14-12-2015
Accepted date: 17-5-2016

Please cite this article as: Dagmara Kulesza, Paulina Bolek, Adrie J.J. Bos, Eugeniusz Zych, Lu_2O_3-Based Storage Phosphors. An (In)harmonious Family, *Coordination Chemistry Reviews* (2016), http://dx.doi.org/doi: 10.1016/j.ccr.2016.05.006.

Lu_2O_3-Based Storage Phosphors. An (In)harmonious Family

Dagmara Kulesza[a], Paulina Bolek[a], Adrie J. J. Bos[b], Eugeniusz Zych[a,*]

[a]Faculty of Chemistry, University of Wroclaw
14 F. Joliot-Curie Street, 50-383 Wroclaw, Poland

[b]Delft University of Technology, Faculty of Applied Sciences
Dep. of Radiation Science and Technology (FAME-LMR)
Mekelweg 15, 2629 JB Delft, The Netherlands

[*]corresponding author: eugeniusz.zych@chem.uni.wroc.pl

Contents

Highlights

- Current trends in research on energy storage materials is reviewed
- Properties of Lu_2O_3-based family of storage and persistent phosphors are presented
- Effect of co-dopants on properties of Lu_2O_3:Tb and Lu_2O_3:Pr is discussed
- Possibility of controlled energy releasing by optical stimulation is presented

Graphical Abstract

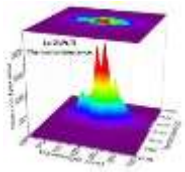

ABSTRACT

Ceramics of Lu_2O_3 activated with either Tb^{3+} or Pr^{3+} and co-doped with one of the transition metal ions – Ti, Hf or Nb - were investigated for their energy storage properties. Photoluminescence, thermoluminescence (TL) and optically stimulated luminescence spectra were recorded and discussed together with thermoluminescent glow curves. The Pr^{3+} and Tb^{3+} ions constitute luminescent centers and participate in the energy storage. However, as the thermoluminescence glow curves showed, the Ti, Hf and Nb co-dopants have a significant impact on glow curve pattern, in particular on the temperature at which the maximum thermoluminescence occurred. For the Tb,Ti and Pr,Ti as well as for the Pr,Nb one main TL peak appeared around 360-370 °C. For other compositions it varied from 210 °C for Tb,Nb, through 230 °C for Tb,Hf to 250 °C for Pr,Hf. In either case additional TL components of lower intensities were observed. They spread over 50-450 °C. The TL data led to the conclusion that the co-dopant – a necessary component to induce a significant energy storage capacity in the materials – may not be directly involved in trapping the excited carriers. Instead, it may rather generate other point defects which, individually or as clusters, would do the work. Energy storage was found to be connected with an appearance of an induced excitation/absorption band spreading over around 350-500 nm and peaking near 400 nm. A prolonged stimulation into this band caused green (for Tb-series) or red (for Pr-series) optically stimulated emission. Such a stimulation allows entirely bleaching out the induced absorption. The optically stimulated luminescence for all members of the Tb-series led to luminescence from both C_2 and C_{3i} sites offered by the host lattice. All compositions of the Pr-series produced optically stimulated emissions upon 400 nm radiation only by means of the Pr^{3+} occupying the C_2 site.

Keyword: thermoluminescence, optically stimulated luminescence, energy storage, defects, Lu_2O_3

1. Introduction to energy storage materials

Luminescence is emission of light by a substance which does not result from its heating. It is thus obvious that emission of luminescent photons, usually visible ones, though they may also appear in UV or IR part of the spectrum, requires delivery of energy to the system. Depending on the type of excitation energy, luminescence may be divided into a whole set of types [1]: photoluminescence (PL), electroluminescence (EL), cathodoluminescence (CL), chemiluminescence (ChL), mechanoluminescence (ML), radioluminescence (RL) or scintillation, thermoluminescence (TL). Practically, all these categories of luminescence find applications, either broad, for example PL in lighting, or more specialized, like in medical imaging or in detection of high-energy particles in high-energy physics experiments.

Many luminescent materials exhibit an afterglow effect i.e. luminescence lasting after ending the excitation. The phenomena is a gradual release of the excitation energy by radiative recombination, which can last anywhere from milliseconds to minutes or even hours after the excitation stimulus has stopped. This occurs especially frequently if the excitation is realized by high-energy radiation – γ- or X-rays, cathode rays, α-particles or just UV photons. It may, however, also appear as a result of irradiation with visible light. Usually, it is considered a drawback of luminescent materials. Yet, if sufficiently long and intense, such a persistent afterglow may be very useful to keep objects visible in dark, during electricity failure for example. The applications are, however, broader and comprise also glowing road signs, watch dials, toys or cloth in which the persistent luminescence serves as an adornment [2]. More sophisticated applications include fibre optic thermometers [3]. This is especially useful if the effect can appear upon exposure to sunlight and/or artificial light. Yen, a pioneer in the field of systematic modern research on persistence phosphorescence, may be considered the first researcher who developed a truly systematic approach to customize the color and duration of glow of persistent phosphors [4]. He claimed that the applications of such materials are still limited by our own imagination.

More recently an increasing interest is focused on nanoparticulated long-wavelength emitting, presumably in IR part of the spectrum, persistent phosphors for use in medical imaging. Thus, persistent luminescence and phosphors presenting such an effect are of increasing interest.

Persistent phosphors emit light for hours after ceasing their irradiation. Since regular luminescence of the emitting centers decays within fractions of seconds (typically from ns to ms) it is obvious that after absorption the energy is first stored in a kind of energy-reservoir from which it is being continuously delivered to the emitting center to excite it and thus allowing its emission of photons. It is nowadays commonly accepted that the energy-reservoirs are host lattice defects (either intrinsic or extrinsic) having ability of immobilizing excited electrons and/or holes. Such defects have filled electronic states above the host

lattice valence band (hole traps) or empty states below the valence band (electron traps). Fig. 1 presents a scheme of electronic states involved in energy trapping and generation of the persistent emission. The distance from the electron and hole energy levels to the relevant bands are defined as the activation energy or trap depth. Usually, upon high-energy photons (X-rays, γ-particles, UV and others), electrons from the valence band are elevated to the conduction band or even kicked off from their mother atoms. In either case, this is proceeded by a thermalization process, where the excess of the excitation energy is removed either via multiple-center excitation or non-radiative energy dissipation. Such excited carriers either recombine directly at a luminescence center or fall down to the trapping sites. The trapped carriers may be liberated by two main mechanisms: i) taking advantage of lattice vibrations or ii) by optical stimulation. In the case of i) depending on the traps energies (traps depths) the carriers may get liberated at room temperature (RT) or, for deeper traps, after additional heating to higher temperatures. If that happens at RT an afterglow or persistent luminescence is produced and the novel persistent phosphors are capable of producing such emission for a whole night and even longer [5]. The intensity and duration of persistent emission are obviously dependent on the population of the trapped carriers and this in turn on the population of effective traps. Note, that for traps deep enough to keep the carriers at RT for a very long time the afterglow or persistent emission are basically absent. Yet, a fraction of absorbed energy goes, during the first stages of irradiation, to the traps so the instantaneous luminescence is less efficient than it might be if the traps were not present. The energy (exited carriers) trapped in such deep traps may be liberated upon heating and then thermoluminescent photons are being produced. This may occur as the carriers freed from their traps diffuse to the emitting centers where they excite these centers. Their subsequent de-excitation produces the TL emission.

Persistent, energy storage and dosimetric materials are different in some aspects. Yet, they share the physics standing behind all the processes related to energy storage and its subsequent recovery/release. Namely, in all those materials excited electrons and holes left behind them must be captured and immobilized in metastable trapping electronic states positioned deeply enough compared to the bottom of conduction band (electron traps) or the top of valence band (hole traps) to not let those carriers to escape too quickly.

For persistent phosphors the traps are still shallow enough to allow the captured carriers to free them continuously at room temperature taking advantage of the host lattice vibrations. This permits for light generation as long as the traps releases the carriers. In the case of storage phosphors and dosimetric materials the traps have to be deeper as ideally they should not lose the carriers at room temperature at all. Consequently, they can be read out deliberately by an external stimulation (thermal or optical) at any, even very long, time after the carriers trapping.

The complexity of the mechanism of thermoluminescence is well illustrated by the fact that even nowadays it is one of the least understood luminescence processes. On the other hand indeed a great progress has been made in this field within last twenty years. Intriguingly, the effect of energy storage resulting in generation of persistent emission was not only observed but deliberately exploited for the first time not later than in 140-88 B.C. This we know from a Chinese publication dated in the Song dynasty (960-1279). In that text a painting with a cow grazing outside is described. Yet, in dark the same painting presented the cow in a cowshed [6,7,8]. This effect could obviously be obtained using a paint or ink containing a persistent phosphor, the light from which produced the night-specific picture after dusk. Whatever the persistent luminescence material was, it was the first artificially prepared phosphor to which a written document refers. A great number of equally intriguing stories the reader may find in a fascinating book by Harvey [9]. Here, let us yet refer shortly to the history of Bologna stone. It was discovered in 1603 by Vincenzo Cascariolo, a cobbler, in Volcanic rock of Mount Paderno near Bologna, Italy [10]. After heat-treatment and exposure to sunlight it could then glow in dark for hours. At that time, it was a real mystery and the discoverer hoped that he found the Philosopher's Stone. It took some 400 years to understand that Cascariolo found a barite, $BaSO_4$. This, heat-treated at reducing atmosphere got converted to BaS and the impurities it contained, like Cu, granted the described glowing in dark. Nowadays, Cascariolo is considered the discoverer of a first persistent phosphor in Europe. At that time the property of Bologna stone was absolutely astonishing and attracted attention from many. The best proof for that may be found in Goethe's "The Sorrows of Young Werther", where we can read: "It is said that the Bonona stone, when placed in the sun, attracts the rays, and for a time appears luminous in the dark"[11].

Almost equally accidental were many later discoveries of persistent and storage phosphors till the end of XX century. Among them, the most efficient was ZnS activated with Cu^{+} discovered in 1920 and next further improved in efficiency and duration of the persistent emission by co-doping with Co^{2+} [12,13,14]. A special role in the development of understanding of the energy storage processes is connected with a research on the alkaline earth metals (M) aluminates, MAl_2O_4, activated with lanthanide ions. In 1966 Lange [15] and Abbruscato in 1971 [16] reported on a bright green luminescence followed by a significant afterglow in $SrAl_2O_4:Eu^{2+}$]. Similar results were reported for analogous compositions with Ca and Ba by Blasse and Bril in 1968 [17]. At that time, all those observations were very disappointing, as the afterglow precluded practical application of these phosphors in lighting.

Everything changed in 1996, when Matsuzawa greatly enhanced both the intensity and duration of the afterglow in $SrAl_2O_4:Eu^{2+}$ by co-doping with Dy^{3+} [18]. Its persistent luminescence was extended to 10-15 hours which opened a different part of the market for those aluminates. Co-doping of the MAl_2O_3:Eu with Nd was also greatly successful and led to the persistent emission lasting for 10 hours. This number was soon tripled. Takasaki and Lin also significantly contributed to the research on aluminates at that time [19,20]. Soon, a

whole family of silicates, $M_2MgSi_2O_7:Eu^{2+},Dy^{3+}$ (M = Ca, Sr, Ba) was proved to exhibit equally significant persistent luminescence. And also in this case, Nd co-doping (instead of Dy) led to efficient persistent luminescence lasting for many hours [21,22,23]. An important impact to the research on novel persistent phosphors was made by Yen [4,24,25,26,27,28], whose systematic exploration of "glow-in-the-dark" materials allowed the accumulation a broad experimental data on properties of such phosphors and, importantly, factors affecting them.

The newly discovered reasonably priced persistent phosphors replaced the previously used sulfides. They are now used among others in watch hands, glowing textiles and T-shirts, luminescent paintings, but also in specific waveguides, thermometers, detectors of micro-defects or detectors of ionizing radiation [18,29,30,31,32,33,34]. Parallel to the market-oriented research those spectacular discoveries launched a systematic research on the phenomenon in the aluminates, silicates and other compositions.

An important part of the history of the research on the energy storing materials is connected with the discovery of this effect in $BaFBr:Eu^{2+}$ and its broad use in the digital radiography [35]. It took almost two decades to figure out what is the detailed mechanism of the effect in this composition and the findings were nicely reviewed by Schweizer [36] and Leblans [37]. It turned out that fluorine "antisites", thus fluorine in bromine position, played very important role in F center generation and the latter is involved in the efficient energy storage. It is nowadays commonly accepted that point defects are the necessary constituents of energy storage materials to form metastable states capable of immobilizing excited carriers, electrons and/or holes.

The prerequisite for storage phosphors and dosimetric materials is the presence of traps deep enough to efficiently keep the acquired energy at room temperature. Yet, there are also requirements which differentiate these two groups of phosphors. Storage phosphors are often used in imaging systems. Thus, they are read out shortly after irradiation and usually it is enough if the fading of the signal is negligible within minutes or hours. In contrary, dosimetric materials often collect the incoming energy in small portions but during a long time – days, weeks or months, even years. Consequently, the leakage of the already trapped carriers has to be strongly limited, and ideally it should be absent. Furthermore, since dosimetric materials are mostly used to monitor the dose people could be exposed to an important requirement is that their effective atomic numbers (Z_{eff}) are close to the effective atomic number of water, the main component of human body. This ensures a comparable energy dependence of interaction of X-rays with both the dosimeter and body of monitored persons. For LiF the Z_{eff}=8.2, while for H_2O it is 7.4. Only a limited number of compositions fulfil this expectancy being simultaneously efficient in energy storage. One of the most prominent examples are dosimeters based on LiF. They are used in two main modifications: LiF:Mg,Ti (MTS) and LiF:Mg,Cu,P (MCP) [38,39,40]. The former is utilized in standard dosimetric procedures, while the latter has extraordinary sensitivity and can be applied for reading low doses of ionizing radiation [41]. The MCP version is able to read

doses down to 50 nGy, which makes it by about 200 times better than the standard MTS. The LiF dosimeters produce thermoluminescent light after exposure to ionizing radiation due to formation of stable color centers. One of them, F_3^+, emits at 530 nm while 640 nm emission is related to F_2 center [42,43]. Other important dosimetric materials are Al_2O_3:C, $CaSO_4$:Dy, MgB_4O_7:Dy, MgB_4O_7:Gd,Li, BeO etc. [41,44,45,46,47,48,49]. However, those based on LiF, and MgB_4O_7 having the density of ~2.65 g/cm^3 and 2.53 g/cm^3, respectively are the most tissue equivalent, and therefore they are so commonly used in dosimetry. BeO has only a slightly higher density (3.02 g/cm^3), but it is highly toxic, which limits its use. Other compositions are usually denser.

The importance of density, chemical composition and effective atomic number (Z_{eff}) of dosimetric materials is clear from Fig. 2 presenting the dependence of attenuation coefficient [50] on energy of the ionizing photons of two such materials: LiF and presented broadly in the next part of this paper Lu_2O_3. While the former absorbs pretty evenly particles of all energies, soft and hard X-rays as well as γ-rays, the latter strongly preferentially absorbs the lower-energy photons. In dosimetry, such a characteristics lead to very much overestimated response to the low-energy ionizing photons compared to the more energetic ones. LiF, with its low density and low effective atomic number (~8.2) behaves very much like human tissues. Thus, the high density of Lu_2O_3 (9.4 g/cm^3) and its high effective atomic number (67.3) makes it much more suitable for imaging than for dosimetry. However, it was also shown that a combined use of both low-Z and high-Z dosimeters could be of great importance to determine the incoming radiation quality/energy quickly and reliably [51,52]. For that the higher the difference of effective Z numbers of both dosimeters the better assessment of radiation quality can be made.

All the positive properties of LiF as dosimeter are accompanied by two significant drawbacks. First, the fluoride is hygroscopic and precautions have to be made to preclude any longer contact of the material with air, not to say with water. Second, after each thermoluminescent reading it has to be subjected to a special heat-treatment procedure to reactivate its energy-storage capability [53,54]. This, obviously, makes its use somewhat complicated. Nevertheless, the mentioned difficulties are not so sever to distract the LiF dosimeters from a broad practical exploitation.

While for years energy storage properties were hardly understood (to say the least), last 20 years brought a great progress in the understanding of this phenomenon [21,22,23]. Consequently, nowadays there are at least a few compositions whose abilities of energy trapping were first predicted and then experimentally confirmed [55,56,57,58,59]. This was possible after an in-depth understanding of persistent luminescence mechanism in such novel, highly efficient persistent phosphors as $SrAl_2O_4:Eu^{2+},Dy^{3+}$, $CaAl_2O_4:Eu^{2+},Dy^{3+}$, $CaAl_2O_4:Eu^{2+},Nd^{3+}$ or in silicates [18,60,61].

A great help in a rational analysis of the persistent luminescence mechanism was possible using the procedure of locating energy levels of Ln^{3+} and Ln^{2+} ions within the energy gap of

the host lattice proposed by Thiel [62,63] and developed into a semi empirical theory by Dorenbos [64,65,66]. Recently, Dorenbos has been extending this concept into d-elements [67,68]. The beauty of Dorenbos concept is that it is enough to know the location of the ground state of just one lanthanide ion, Ln^{3+} or Ln^{2+} against the valence and conduction bands of a defined host lattice to conclude about the location of ground states of all other lanthanides. The Dorenbos approach is both simple and elegant and it was proved to be effective in analysis of thermoluminescent properties of some compositions [55,56,57,58,59]. A similar work for d-elements proved a much greater complexity of the problem. Yet, an important finding was that energy of electron transfer from the surrounding ligand (so from the valence band) to the Ti^{4+} is always very close to such an energy for Eu^{3+} in the same host [68]. Consequently, some predictions of positions of the Ti^{3+}/Ti^{4+} levels in various compositions is possible as Eu^{3+} CT states are known for a vast number of hosts. It also allows for a better understanding of the luminescent properties of Ti in various hosts [69,70,71]. Nevertheless, evaluation of the role of d- or closed-shell elements in energy trapping and in thermoluminescence processes is still a challenge and there are no efficient and universal theoretical tools for that.

There is no doubt that Dorenbos approach boosts the research on the persistent and storage phosphors, nowadays. Yet, it is also obvious, that this concept does not explain all the complex properties of those materials. The mechanisms of energy storing and its controlled recovery are often mysterious and puzzling. Thus, the simple scheme shown in Fig. 1 presents indeed only a general outline of the mechanisms. For example, in some materials, also tunnelling may occur, either the classic or a temperature dependent one [72,73,74,75,76,77]. It is very desirable to combine a set of different spectroscopic techniques to get possibly thorough, comprehensive picture of the processes occurring in a specific composition.

From Fig. 1 and the Dorenbos model we discussed above, it is clear that the traps' depths are defined by the dopants (defects) introduced into the host material. It was, however, shown in recent years that the trapping capability of defects may be altered and well controlled by changes in the composition of the *host material* and especially comprehensive research in this field have been performed for garnets [78,79,80,81,82,83]. They show efficient photoluminescence and scintillation but suffer from afterglow, which was recognized to result from so-called antisite defects [84,85,86] developed during crystal growth from melt. These defects are formed when Y^{3+} enters Al^{3+} site and vice versa [78]. This leads to generation of electronic defect states (DS) below conduction band of the host which serve as electron traps, see the scheme in Fig. 3. They are typically shallow enough to release the trapped electrons at RT. Consequently, the carries become available for generation of emission photons with some delay which is seen as afterglow. Partial substitution of Al with Ga in $Lu_3Al_5O_{12}$ or $Y_3Al_5O_{12}$ moves the bottom of the conduction band to lower energies (Fig. 3). Effectively, it makes the trapping sites even shallower at first and, with still larger substitution of Al with Ga, immerses the DS within the host conduction band

and thus deactivates the defect trapping capability. Consequently, the delayed emission is no longer generated as all electrons raised to conduction band become available for recombination without any delay. This method of reducing or removing an afterglow is termed band gap engineering.

Although, as we mentioned above, the composition is of great importance in the case of persistent and storage phosphors, equally essential is the fabrication process and its parameters. This was already confirmed by us for Lu_2O_3:Tb,M (M=Ca, Sr, Ba) ceramic persistent phosphors [87,88,89,90,91]. Prepared in air did not produce any thermoluminescence, while made in vacuum, and especially in a more reducing atmosphere of a forming gas they produced a persistent green emission lasting for hours. What is more, the effect needed a heat-treatment at about 1700 °C as preparation at did not give any significant afterglow. Thus, composition – qualitative and quantitative – has to be precisely optimized *together* with the fabrication process parameters to develop the specific persistent/storage phosphor potentials. These may be easily overlooked as we proved recently in the case of $LuPO_4$:Eu [92,93].

It was postulated that in Lu_2O_3:Tb,M (M=Ca, Sr, Ba) ceramics Oxygen vacancies ($V_O^{\cdot\cdot}$) were involved in the energy trapping [87,88,89,90]. At that time, seeking the possibility to reduce/get rid of the afterglow or persistent emission in Lu_2O_3:Tb,M (M=Ca, Sr, Ba) we prepared Lu_2O_3:Tb,Hf and Lu_2O_3:Pr,Hf ceramics. We supposed that the Hf co-dopant would suppress the population of $V_O^{\cdot\cdot}$ and consequently remove the persistent luminescence effect [90]. Indeed, in Lu_2O_3:Tb,Hf or Lu_2O_3:Pr,Hf ceramics the afterglow was practically not observed. Yet, it soon appeared that the ability of energy storage in the Hf co-doped composition was still present but the traps were deep enough to immobilize the excited carries at room temperature for a much longer time. In practice the carriers were permanently stored in traps at RT and could be released only by an external thermal stimulation up to about 200-300 °C. Thus, changing the co-dopant from M^{2+} ions to Hf^{4+} replaced the relatively shallow traps, presumable connected with $V_O^{\cdot\cdot}$ sites, into deeper ones, supposedly linked to the Hf^{4+} in the Lu^{3+} positions ($Hf_{Lu}^{\bullet}$). As we shall see later, in the light of new experimental data this conclusion appears oversimplified.

While obviously the Dorenbos model which we mentioned above cannot be used directly to the Lu_2O_3-based compositions (it does not explain the possible role of the various co-dopants: M^{2+}, Hf^{4+} and others we shall discuss later), it does explain that both Tb^{3+} and Pr^{3+} ions have potential to serve as hole traps transforming from Tb_{Lu}^{X} (Pr_{Lu}^{X}) into positively charged $Tb_{Lu}^{\bullet}$ ($Pr_{Lu}^{\bullet}$). In this paper we shall present a summary on the thermoluminescent properties of the Lu_2O_3:Tb,M and Lu_2O_3:Pr,M (M=Hf, Ti, Nb) persistent and storage phosphors. We shall focus on the similarities between the Tb- and Pr-activated compositions.

2. Experimental

Sintered ceramics of Lu_2O_3:Pr,M (Pr-series) and Lu_2O_3:Tb,M (Tb-series) were prepared from nanocrystalline powders obtained by the classic Pechini method [94,95,96]. Hereafter, the ceramics of the Tb-series with M=Hf will be denoted LTH, for M=Ti it will be LTT and for Nb-co-dopant it will be LTN. Analogously, for the Pr-series the LPH, LPT and LPN will stand for Hf-, Ti- and Nb-co-doped ceramics. In short, for the synthesis of starting powders, stoichiometric amounts of lutetium(III) nitrate pentahydrate ($Lu(NO_3)_3 \bullet 5H_2O$), and appropriate activator - praseodymium(III) nitrate hexahydrate ($Pr(NO_3)_3 \bullet 6H_2O$) for Pr-series and terbium(III) nitrate hexahydrate ($Tb(NO_3)_3 \bullet 6H_2O$) the Tb-series were dissolved in 2 M water solution of citric acid ($C_6H_8O_7$). The co-dopants were then introduced as hafnium(IV) chloride ($HfCl_4$), niobium(V) chloride ($NbCl_5$) and titanium isopropoxide ($Ti[(OCH)(CH_3)_2]_4$). Such a solution was combined with some ethylene glycol ($C_2H_6O_2$) as a complexing agent. The solution was slowly heated up to 180 °C at which temperature a solid resin was formed. Next, the temperature was gradually increased to 700 °C and held for 5 hours to burn off the organics. Finally, portions of each powder, ~0,25 g, were pressed into pellets under the load of 4 tons for 5 minutes and were transferred to a tube furnace. The heat-treatments were performed at 1700^{o}C for 5 hours in forming gas of 25% H_2 and 75% N_2. The heating and cooling rates were 3 °C per minute.

Crystallographic purity of all ceramics was checked by means of powder X-ray diffraction (XRD) analysis in the range of 2ϑ = 10–80 degree using a D8 Advance diffractometer from Bruker. Excitation and emission spectra were recorded using FLS 980 spectrofluorometer from Edinburgh Instruments using a 450 W Xenon arc lamp as an excitation source. Excitation spectra for the Pr-series were monitored at 631.5 nm luminescence and for the Tb-series at 542 nm. Typically, in such measurements the emission monochromator slits were set at 1 nm. Excitation spectra were recorded at room temperature for raw (non-irradiated) materials, then after irradiation with 270 nm (for Tb-series) or with 280 nm (for Pr-series) for 10 minutes and after the 270/280 nm radiation *combined* with prolonged (20 min) stimulation of ~400 nm afterwards.

TL glow curves were registered using RISO TL/OSL reader model DA-15 and controller model DA-20. Samples were irradiated with $^{90}Sr/^{90}Y$ β-source with a dose rate of 0.7 mGy/s. Measurements were performed in nitrogen gas atmosphere with a heating rate of 5 °C/s. Emission registered during TL measurements was detected using an EMI 9635 QA photomultiplier tube (PMT). It was found that thermoluminescent properties of all the compositions after irradiation with 254 nm or 270-280 nm are very similar to those after exposure to β-rays.

3. Results and discussion

Fig. 4a presents photo of a pellet prepared by cold-pressing of the as made powder and its sintered version. Fig. 4b shows a microstructure of the starting powders made by the Pechini method and Fig. 4c presents a typical microstructure of the sintered ceramics

fabricated at 1700 °C. It appears that sintering leads to a significant shrinkage of the ceramic body and affects the ceramics microstructure. The small, basically nanosized crystallites of the as-made powders grow into large micron-sized grains during sintering. Thus, the heat-treatment causes a great mass transfer and the grains in the sintered ceramics are being formed atom by atom practically from scratch upon the high-temperature processing. It is important, as according to [97] sintering of commercial powders made of much larger grains does not give ceramics with any significant TL. Thus, the capability of energy storage we shall be discussing later in this paper is caused by both high-temperature treatment and significant mass flow during the high-temperature processing. This is assured only when the starting powder is composed of nanosized particles.

The changes in the microstructure caused by the high-temperature sintering are also seen in XRD patterns presented in Fig. 5. While both the as-made powder and the sintered ceramics show only lines related to the cubic structure of Lu_2O_3, the diffraction lines of the former are much broader than for sintered pellets. This indicates a significant growth of crystallites and is in agreement with the changes in microstructure just presented in Fig. 4.

TL glow curves for Lu_2O_3:Tb,M (Tb-series) are presented in Fig. 6a. All curves cover a wide range of temperatures, starting from 50 °C till 400 °C, and for Ti co-doped material the TL extends up to about 450 °C. Each of the glow curves presented in Fig. 6a possesses a dominant TL band. For LTN composition it is localized at about 210 °C, for LTH around 250 °C and for LTT around 365 °C. It is thus enticing to connect the change in the positions of the TL peaks with the change of the co-dopant, which would further imply that the trap depth is defined by the co-dopant, while the activator would serve as a recombination center and produce thermoluminescence. Undoubtedly, the shapes of the TL curves varies which proves that the co-dopant strongly affects the population of specific energy traps in Lu_2O_3:Tb,TM ceramics. The high-temperature TL of LTT sample can be taken as an advantage at first, as the deep trap(s) should be able to store energy for long time without any significant fading. Yet, this is also connected with rather high thermal quenching of the luminescence of Tb^{3+}, which we shall deal with later in the paper. Consequently, this may translate to rather inefficient conversion of the stored energy to the TL photons and we shall see shortly that it is indeed the case of LTT.

An analogous comparison of the Pr-series of compositions makes it clear that the situation is much different (Fig. 6b). Firstly, within TL curve of the LPH samples we see as many as four significant TL peaks. Nevertheless, the dominant component appears at ~220 °C, which is quite similar to the LTH sample (Fig. 6a). In the case of the Nb co-doped system (LPN) the TL main peak is located at 365 °C, which is well-above the most significant TL for the LTN composition. Yet, the TL glow curve of LPN is very much similar to the one produced by the LPT composition with the difference that the latter contains also a shoulder on the main TL band at around 410 °C. Despite the most significant TL components some satellite TL peaks are also observed for practically all compositions. These may also be noted in singly doped

compositions (Lu_2O_3:Tb and Lu_2O_3:Pr) whose TL were found to be of very low intensities, however [98,99,100]. Still, the simplest structure of the components is seen for the LPT ceramics, as virtually it is made up of one band peaking at 365 °C with the mentioned shoulder on its high-temperature part.

Comparing all the TL glow curves of Tb- and Pr-series of ceramics we may easily note that basically for each composition a very similar set of TL components (thus traps) is observed and just their individual contributions to the overall TL strongly vary from composition to composition. Yet, there is one exception from that, as both the LTT and LPT ceramics produce basically the same TL glow curve and, as already mentioned, it coincides with the glow curve of LPN.

At the present stage of their development the Lu_2O_3:Tb,Hf ceramics seems to outperform all the others Lu_2O_3-based storage phosphors. Thus, in Fig. 7 we compare the TL glow curves of the Lu_2O_3:Tb,Hf and the commercial BaFBr:Eu. The integrated intensity of the LTH ceramics reaches 65 % of the BaFBr:Eu TL. We take it as a promising result especially that no correction for the temperature quenching – significant in LTH as will be seen later - was applied for these calculations.

Fig. 8 presents the comparison of the TL emission spectra of Tb- (Fig. 8a) and Pr-series (Fig. 8b) taken at the temperature of TL peaks. It is evident that Tb and Pr are the only emitting centers in the two series of ceramics. Presumably, this means that the activators serve as the recombination centers for the excited carriers escaping their traps. Moreover, the observed emissions result from either the $^5D_4$ level (Tb-series) or $^1D_2$ (Pr-series) giving either green or red color thermoluminescence, respectively. Also RT photoluminescence upon excitation into the f→d band of either of the activator does not contain components related to transitions from any higher energy levels of the activators. For the case of Pr the lack of luminescence from its $^3P_0$ level was researched both experimentally [101] and theoretically [102] as such a luminescence would be very desirable for scintillation purposes [103]. Let us yet note that, in principle, the electron-hole recombination might take place at a hole-trapping center adjacent to Pr/Tb and only afterwards the energy would be transferred to the activator which would then produce luminescent photons. Yet, in light of the current experimental data such a process does not seem likely as it was already claimed that these are the activators, Pr^{3+} or Tb^{3+}, that serve as the hole-trapping centers. Thus, the electron-hole recombination can be reasonably expected to occur *directly* at these dopants [90].

As seen in Fig. 8, for the Tb-series (Fig. 8a) the highest-intensity thermoluminescence is produced by LTH material. This appears to be by the factor of 12 higher than TL from the LTT ceramics and by a factor of about 3 stronger than TL of the LTN composition. Yet, these numbers reflect the TL intensities at temperatures which are much different for the three specimens, as their most intense TL appears at much different temperatures. Thus these numbers do not reflect the ratios of energies stored by the three ceramics. For a realistic estimation of the energy storage the thermal quenching of the Tb luminescence should be

known. This we measured monitoring intensity of the green Tb^{3+} emission upon the excitation at 310 nm, so into the f-d absorption band. The results for each member of the Tb-series were very similar. Thus, the resultant curve for the LTN ceramics is given in Fig. 9 together with analogous curve taken for the Pr^{3+} luminescence. As it is seen, both the Tb and Pr emissions are strongly quenched as the temperature increases and this effect is significantly stronger for the Tb composition. At 350-370 °C, where the LTT ceramic shows its highest thermoluminescence, the Tb emission reaches only about 2-3 % of its value at room temperature. At 210 °C, a TL maximum for LTN, the thermal quenching reaches about 70 % counted against RT. Pr^{3+} luminescence also suffers from thermal quenching but this is clearly less profound. At ~360 °C, where both the LPT and LPN ceramics show the most intense TL, their photoluminescence still shows about 35 % of the intensity they had at RT. Thus, for both these LPT and LPN ceramics every third of the electron-hole pairs immobilized in their traps indeed contributes to the TL signal.

Thus, simple comparison of the TL intensities measured at so many different temperatures does not bring the answer on efficiency of energy storage but rather on the efficiency of energy recovery by thermal stimulation. Consequently, if we correct the measured TL intensities for the thermal quenching, the efficiency (of energy storage) of the LTT ceramics would reach about 75 % of the efficiency of the LTH. Then, the least efficient in energy storage would be the LTN ceramics, whose capability of immobilizing the excited carriers would be at the level of about 25 % of the most effective LTH ceramics. Therefore, at the present stage of their development, the LTH and LTT ceramics appear to be the most promising for efficient energy storage. Two main reasons for that are: the high efficacy of immobilizing the energy carriers – excited electrons and holes – and thermoluminescence at sufficiently high temperatures to offer a long-term storage without any significant fading. In the later part of this paper we shall see if these hopes harmonise with the reality.

As it comes to the Pr-series, analogous comparison of TL efficiency is presented in Fig. 8. The strongest TL measured at the temperature of TL peak is produced by the LPN ceramics, while the LPH and LPT samples perform by an order of magnitude less efficiently. Taking into account the thermal quenching the *storage* efficacy is by a factor of about 15 higher in LPN than in LPH. Thus, at the present stage of the material's development the LPN ceramics present the highest potential as dosimetric material.

Despite losing about 65 % of the energy in thermoluminescent reading of LPN, its performance is still significant and encouraging. Its high-temperature TL gives good chances for very low fading even in long-term energy storage. In dosimetric applications a low fading rate is an important requirement. Furthermore, energy recovery may be executed by means of optical stimulation in which the trapped carriers are freed by photons whose energy span

the energetic distance from the trap to the bottom of conduction band, at least. Such experiments with their results and analysis are presented below.

As proved above quite significant fraction of the stored energy is lost during the thermal stimulation of both the Tb- and Pr-series. As we already noted, the former one suffers from that effect much more. Yet, for both series the thermally induced nonradiative relaxation is significant. Thus, optically stimulated luminescence (OSL) appears an interesting alternative for TL. The advantages of OSL include not only the lack of thermal quenching but it also may offer to selectively empty the specific traps by properly selected energies of the stimulating photons. Thus, OSL can be of interest to trace the physics standing behind the energy storage properties of the materials. However, the reader should be aware that optical trap depth differs from the thermal trap depth and the relation between them is not straightforward to say the least. Nevertheless, TL and OSL experiments may nicely complement each other to produce a more comprehensive picture of the processes occurring in storage phosphors/dosimeters.

Fig. 10 presents the excitation spectra of the Tb-series of samples. For each composition a raw (unirradiated) samples was measured, than the sample was irradiated with short-wavelength UV (270 nm) and the excitation spectrum was again taken. Finally, the later was additionally irradiated with 400 nm radiation for 20 minutes and then the excitation spectrum was again recorded. The results are given in Fig. 10a for LTT, Fig. 10b for LTH and Fig. 10c for LTN ceramics. The emission was always monitored at 542 nm, thus within the $^5D_4 \rightarrow {}^7F_5$. The spectra, not surprisingly, have common features for all the compositions. Consequently, each of them consist of a broad band in the 230-320 nm range of wavelengths, which reflects the spin-allowed $4f^8 \rightarrow 4f^7 5d^1$ ($f \rightarrow d$) transition. One can also note a weak broad band resulting from a spin-forbidden $f \rightarrow d$ transition around 350 nm [104,105]. It is superimposed on the weak, narrow and parity-forbidden f-f transition of Tb^{3+} in this range of wavelengths. Above 475 nm a next series of f-f transitions related to the $^5F_6 \rightarrow {}^5D_4$ excitation is observed. Already comparing the spectra of the unirradiated ceramics we see that for the LTT one the band in the 250-325 nm range of wavelengths has clearly different intensity ratio of the components compared to the LTH and LTN samples. In LTT the component around 310 nm is always relatively stronger than for the other two ceramics. This may reflect that an absorption (excitation) connected with the Ti co-dopant is located in this area and it also contributes to the Tb luminescence. This might be an $O^{2-} \rightarrow Tb^{4+}$ charge transfer transition, whose position could be reasonably expected in this range of wavelengths. A closer examination of the spectra of the other two ceramics proves that also in the case of the LTN sample the 310 nm component is clearly stronger than in the LTH. And this is reasonable as the similar $O^{2-} \rightarrow Nb^{5+}$ CT transition should appear at such moderate energies while the $O^{2-} \rightarrow Hf^{4+}$ CT band should be more energetic. Thus, the excitation spectra of the raw compositions are similar and the differences can be understood and explained as resulting from the slightly different chemical character of the co-dopants.

However, what is the most striking in Fig. 10 is an appearance of a broad band located in the range of near-UV and blue-green part of spectrum for all specimens. Its shape and location slightly vary with the co-dopant. For LTT it seems to cover ~320-480 nm range of wavelengths, for LTH and LTN it is ~370-480 nm range of wavelengths. In fact also for the latter two a less intense component might be seen around 320-370 nm. Altogether, the common effect of irradiation with 270 nm is that in all the ceramics of the Tb-series a new absorption band is generated. This effect is also observed when the samples are irradiated with X-rays. Furthermore, when the irradiated samples are exposed to ~400 nm radiation for 10-20 min afterwards, the just induced excitation/absorption band is fully bleached out and the excitation spectra for either of the ceramics appear practically identical with the ones taken for unirradiated specimens. It is noteworthy that after such a treatment (270 nm+400 nm irradiation) the samples do not show any thermoluminescence. We found that the sequence of irradiations may be repeated many times and the effects are always very similar. Thus, the energy storage is clearly associated with the generation of the UV-Vis broad band absorption.

Despite the similarity of the induced excitation band in the three ceramics of the Tb-series, it is also pretty obvious that the peak position varies to some extent. For the LTT and LTN compositions the band seems to contain two overlapping components as its shape is strongly non-symmetrical for these ceramics. Yet, we tested that total bleaching of this absorption may be achieved by stimulation either at its peak or into the tails of the band. Thus, at present we do not see any difference in the phosphors behaviour, which might be related to the stimulation wavelength/energy as long as it meets the range of the induced absorption.

The presence of the induced absorption is also seen by eye as the samples get slightly brownish in color after irradiation with the 270 nm radiation or with X-rays. Let us note that the enhancement of excitation efficiency below about 300 nm after the 270 nm irradiation is caused by the fact that the traps are generally filled and the absorbed energy is not shared between photoluminescence and trapping processes but is basically used for PL only. Thus, this is not a surprising but rather expected effect.

Let us stress that the appearance of the induced broad absorption around 400 nm in *excitation* spectra entails that stimulation into this band produces Tb^{3+} emission. Since this effect is reversible it also implies that this is the region of wavelengths where by optical stimulation we can release the stored energy. We can then, in other words, use the ~400 nm radiation to read the stored information. All of that at RT, when thermal quenching does not pose a problem (see Fig. 9). This is especially good news as the optical stimulation can be done with energies higher than the emission they cause. Consequently, the discrimination of

the stimulated (scattered) light and the emitted one can be done by standard optical filters. In many storage materials the stimulation is performed by a wavelength longer than the produced emission wavelength. A classic example is $Ba(F,Br)_2:Eu^{2+}$ in which the optical reading is done by a He-Ne laser with its 632.8 nm light [1,35,36] while the emission wavelength is around 400 nm.

An analogous set of measurements was performed for the Pr-series of materials. The results are presented in Fig. 11. The excitation spectra were taken monitoring the 631.5 nm emission, resulting from the $^5D_1 \rightarrow {}^3H_4$ transition. The spectra generally consist of bands resulting from the f→d transitions below about 350 nm and, at longer wavelengths, narrow lines due to the intraconfigurational f-f transitions are observed. Differences which might be connected with the co-dopants are not clearly seen in the Pr-series, though for the LPT ceramics some long-wavelength shift of the f-d band is indeed observed. The changes due to the exposure to the 280 nm radiation are very similar to what was seen for the Tb-series of materials. Thus, again the 280 nm irradiation induces broad excitation/absorption bands located in the range of about 330-450 nm. The new band is also spread over a wide range of wavelengths and offers a convenient way for optical stimulation as around 400 nm Pr^{3+} does not have any absorption. Therefore, for all samples the bleaching was carried out with 400 nm light and for all the ceramics of the Pr-series the excitation/absorption spectra returned to those characteristic for the non-irradiated samples. The effect could be reproduced over and over again proving that storing and reading the information is repeatable. Thus, also in the case of the ceramics of the Pr-series the stimulation around 400 nm allows to release the trapped carries from their traps. The red Pr^{3+} emission is then produced. Hence, the reading of information may be realized by OSL technique in the storage phosphors of the Pr-series, too.

The changes seen in the excitation spectra and induced by irradiation with high-energy photons (Figs. 10 and 11) are mirrored by interesting variations in emissions when excited into the characteristic absorption/excitation bands. Fig. 12 presents luminescence spectra taken upon excitation in the f→d band characteristic for the Tb^{3+} ions occupying the C_2 (thus: having no inversion symmetry) symmetry site of the Lu_2O_3 host located around 270 nm and into the band located around 320 nm which is characteristic for ions of both activators occupying the C_{3i} (centrosymmetric) site. These two spectra are accompanied by the emission produced upon excitation around 400 nm, hence, into the excitation band induced by irradiation with short-wavelength UV or ionizing radiation. In the case of all three compositions of the Tb-series (Fig. 12a,b,c) the pattern is clear and not surprising. Namely, upon excitation at 270 nm (black lines) the relative intensities of the lines in the range of

470-510 nm compared to those around 535-560 nm are stronger then upon excitation at 310 nm. This is reasonable as the more energetic emission is due to a $^5D_4 \rightarrow {}^7F_6$ electric dipole induced transition which is more probable in the case of the noncentrosymmetric site. The lines in the range of 535-560 nm are due to the $^5D_4 \rightarrow {}^7F_5$ transition which becomes allowed in centrosymmetric environment of the emitting ion, thus for Tb^{3+} in C_{3i} site. Consequently, in the range of the $^5D_4 \rightarrow {}^7F_5$ transitions we have an opportunity to observe emissions from both the Tb(C_2) and Tb(C_{3i}) sites. And indeed, a close examination of the 535-560 nm range of the emissions allows to select, even for the RT spectra, lines which are characteristic for the Tb(C_2) ions and those connected with the Tb(C_{3i}) ones. When the excitation is made at 410 nm (or around) the emission spectra of all the compositions of the Tb-series appear to contain lines characteristic for both the Tb(C_2) and Tb(C_{3i}) ions. It is thus clear that Tb ions occupying both sites are active in optically stimulated luminescence and, presumably, in energy storage.

Surprisingly, the picture presented by the various emissions excited at the specific broad excitation bands in the Pr-series is different. The spectra for the three compositions are presented in Fig. 13. The photoluminescence spectra excited at 280 nm, when Pr(C_2) is preferentially, but not exclusively, excited and 320 nm, which favors the Pr(C_{3i}) ions differ significantly within each composition. While they always cover 590-730 nm range of wavelengths the excitation at 320 nm (Pr(C_{3i})) produces clearly richer spectra with clearly present lines hardly seen when the excitation goes mainly to the Pr(C_2) (280 nm). Among others the 280 nm excitation produces spectra with the most potent line peaking at 632 nm, while upon 320 nm excitation the most intense line appears at 621.4 nm. The latter spectrum contains also a characteristic set of three, slightly structured lines of significant intensities in the range of ~592-618 nm. These observations are not surprising, as the two sites offered by the lutetia host should lead to such differences. They were also observed for other dopants, for example Eu^{3+} [106]. What is surprising, however, is that optically stimulated luminescence (OSL) spectra, generated upon stimulation into the induced excitation/absorption band around 400 nm, are practically indistinguishable from the photoluminescence upon the 280 nm excitation, thus characteristic for the Pr(C_2) ions. This is a clear effect as the spectra upon the 280 nm and 400 nm excitation almost perfectly overlap for each composition within the Pr-series. Clearly, the Pr(C_{3i}) ions essentially do not contribute to the OSL and thus they seem to be inactive in energy storage. This is in contrast to what was found for the Tb-series discussed above.

In Fig. 14 we compare how the excitation spectra of the LTH and LPH ceramics changes with the dose of the high-energy UV photons. In the case of the LTH sample (Fig. 14a) the intensity of the induced excitation band around 425 nm clearly increases with the dose and the effect is potent. The response of the LPH on the dose (Fig. 14b) is noticeably different. The ~400 nm band appears much less intense even after long irradiation time (high dose). It

thus appears that the OSL-useful excitation component is much more potent in LTH than in LPH. For the two other pairs, LTN-LPN and LTT-LPT, the results are similar. Clearly, while all the Lu_2O_3-based storage phosphors on which we report here show optically stimulated luminescence, the Tb-activated compositions appear superior compared to the Pr-activated ceramics. For OSL reading of doses the Tb-activated materials appear more attractive at present.

The inability of the Pr(C_{3i}) ions to participate in energy storage is a surprise and the reasons for that are not clear at present. Yet, a similar effect was found in the case of Lu_2O_3:Eu. The difference was, however, that, unlike in the Lu_2O_3:Pr discussed here, the persistent luminescence of the Lu_2O_3:Eu ceramics resulted mostly from the centrosymmetric Eu(C_{3i}) ions [106].

4. Conclusions

The Lu_2O_3:Pr and Lu_2O_3:Tb co-doped with transition metal ions – Ti, Hf and Nb - give two series of novel energy-storage phosphors. For the first time their spectroscopic properties were systematically studied and compared within each series and between the Tb- and Pr-series. A significant effect of the co-dopant, Ti, Hf or Nb, on the thermoluminescent properties of both series of ceramics was clearly observed. Yet, the temptation to connect the energy storage properties directly with the introduced co-dopant via an induced localized energy level, may be a misleading approach. While for the Tb,Nb compositions the most intense TL was observed around 210 °C for the Pr-activated counterpart (Pr,Nb ceramics) it was found around 360 °C. In contrary, for the other two co-dopants, Ti and Hf, the glow curve's pattern varied with the activator (Tb, Pr) to a much lesser degree. A common feature of all samples was a broad band absorption/excitation appearance around 400 nm during the energy storage hence when the samples were irradiated with short-wavelength UV or ionizing radiation. In the Tb-series optical stimulation into this band generated green luminescence from Tb^{3+} ions occupying both the C_2 and C_{3i} sites offered by the Lu_2O_3 host. In contrary, each member of the Pr-series presented optically stimulated emissions only from the Pr^{3+} ions sitting in the C_2 symmetry site. At the present stage of the research the reasons for this discrepancy are not clear. The deepest traps observed from thermoluminescence at temperatures around 350 °C, were found in Lu_2O_3:Pr,Nb, Lu_2O_3:Pr,Ti and Lu_2O_3:Tb,Ti.

Acknowledgements

The authors gratefully acknowledge financial support by the Polish National Science Centre (NCN) under the grant #UMO-2014/13/B/ST5/01535 (decision #DEC-2014/13/B/ST5/01535) and partially by Wroclaw Research Centre EIT+ within the project "The Application of Nanotechnology in Advanced Materials"—NanoMat (POIG.01.01.02-02-002/08) co-financed

by the European Regional Development Fund (Innovative Economy Operational Program 1.1.2).

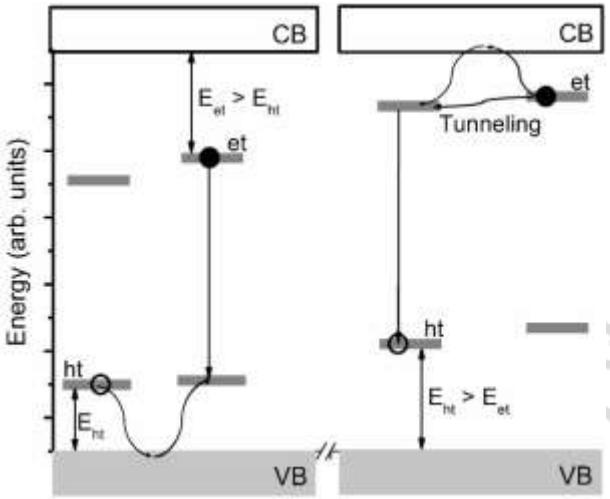

Fig. 1. Schematic depiction of the thermoluminescence processes. The left part presents situation when the hole trap (ht) is shallower than the electron trap (et), while the right part is for the opposite situation. Consequently, in the former the emission results from the electron-trapping center while in the latter from the hole-trapping one.

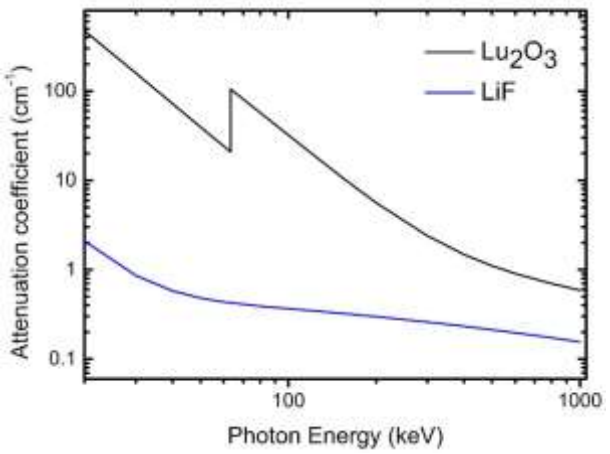

Fig. 2. Attenuation coefficients of LiF and Lu_2O_3 in the range of 20-1000 keV of energy. LiF shows very similar response to the broad range of energies of ionizing radiation, while Lu_2O_3 highly preferentially accumulates energy of the less energetic particles.

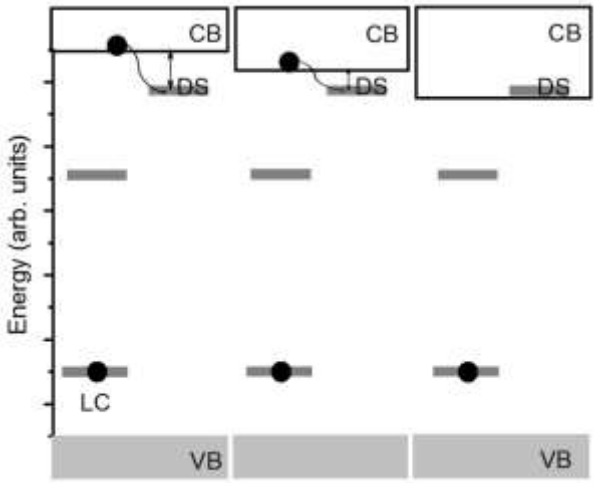

Fig. 3. A simplified scheme of the bandgap engineering and its effect on the energy trapping ability of a defect. From left to right: the lowering of the bottom of the conduction band (CB) reduces the trap depth and finally makes the trap inactive when its energy level locates within the CB. In LuAG and YAG garnets this effect was achieved by partial substitution of Al with Ga. DS stands for a defect state and LC for the luminescent center.

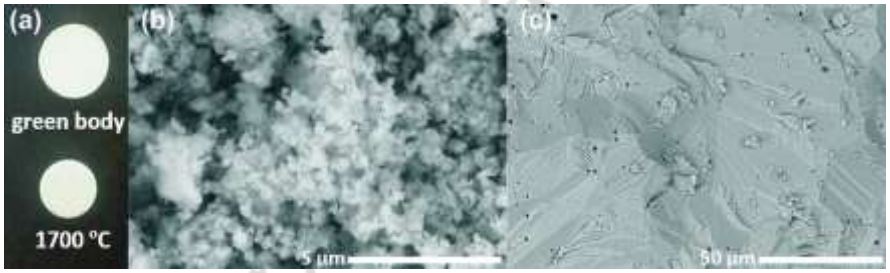

Fig. 4. The appearance of a cold-pressed pellet made of an as-prepared powder (green body) and its sintered version (a). Note the shrinkage of the later due to the sintering. A SEM image of the as-prepared powder (b) and a typical microstructure of the sintered ceramics (c). The results are very similar for all compositions indicating that the small additions of the dopants do not affect the sintering process.

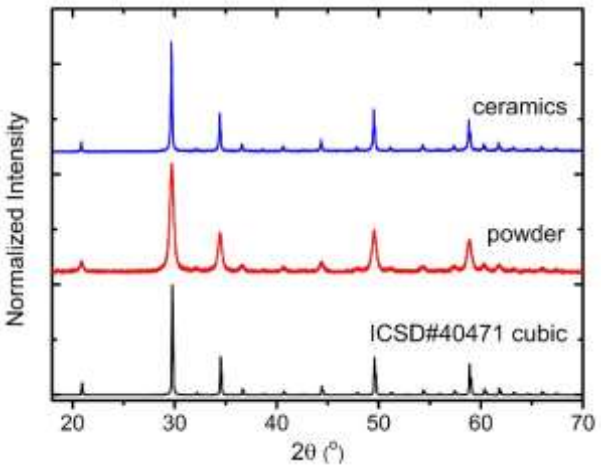

Fig. 5. XRD patterns of the as-made powder (red) and its sintered ceramic version (blue). Simulated pattern for the cubic Lu_2O_3 is given for comparison.

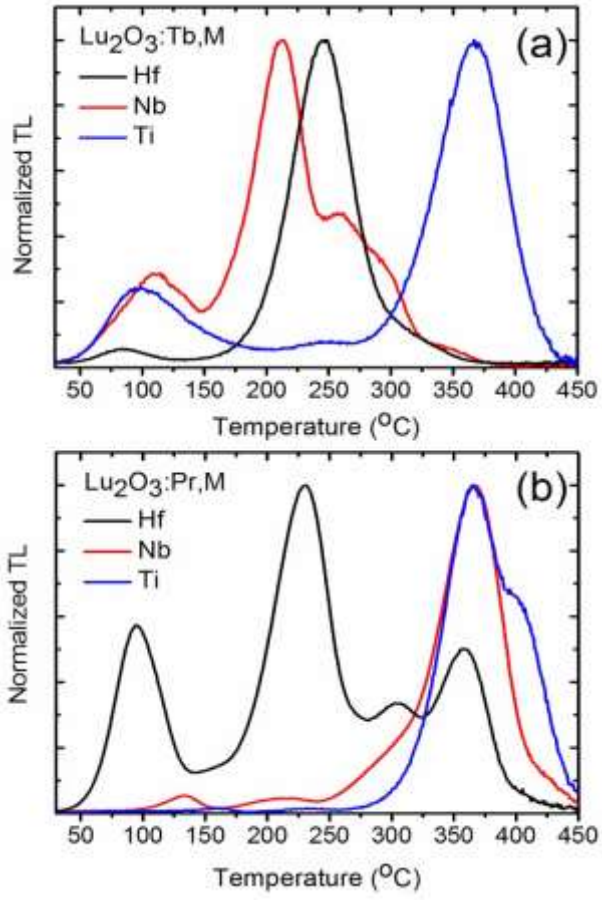

Fig. 6. Comparison of TL glow curves of the ceramics of the Tb-series (a) and the Pr-series (b). The intensities were normalized to the same height of the maxima.

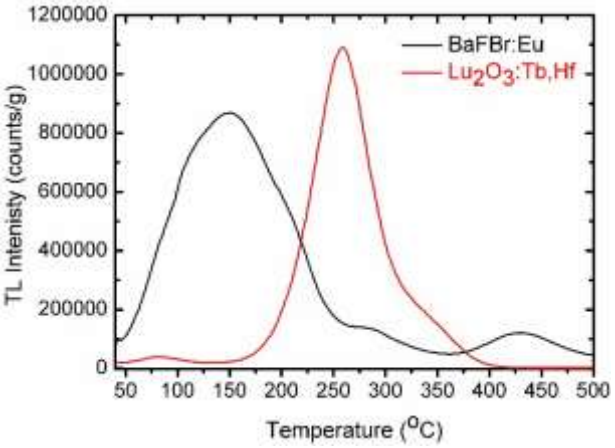

Fig. 7. Comparison of the thermoluminescence of Lu_2O_3:Tb,Hf and a commercial BaFBr:Eu. Intensity of the former reaches 65 % of the commercial storage phosphor TL. No correction for the temperature quenching (see below) was applied.

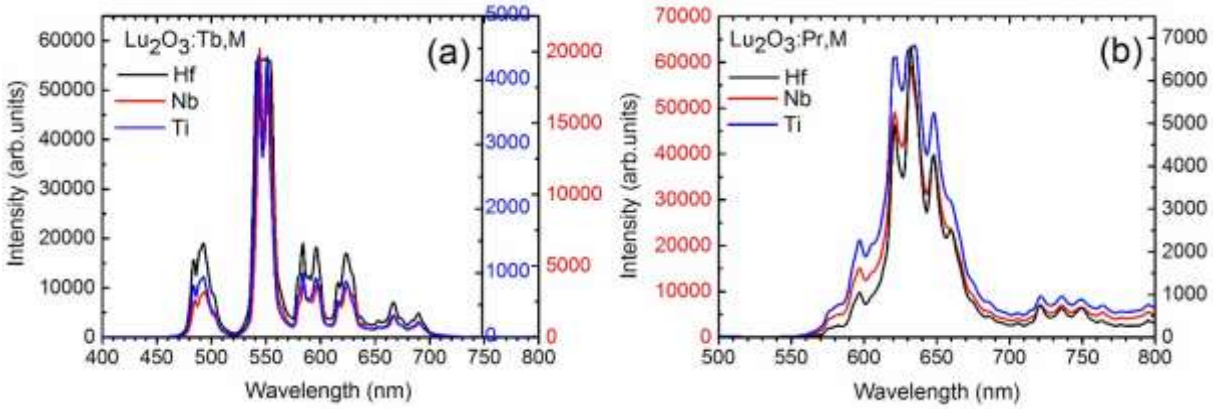

Fig. 8. Thermoluminescent emissions for the Tb- (a) and Pr-series of ceramics (b). Only the activators produce the thermoluminescent photons in both series. In (b) the right Y-axis is common for the Hf and Ti co-doped samples.

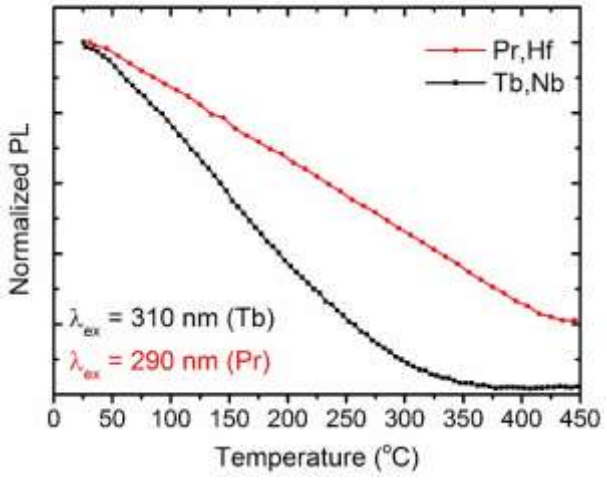

Fig. 9. The exemplary dependences of the PL intensity of the Tb and Pr emissions as the function of temperature. Co-dopants do not alter the courses of both curves in any significant manner, so the other curves are not presented. Both PL curves are normalized at RT.

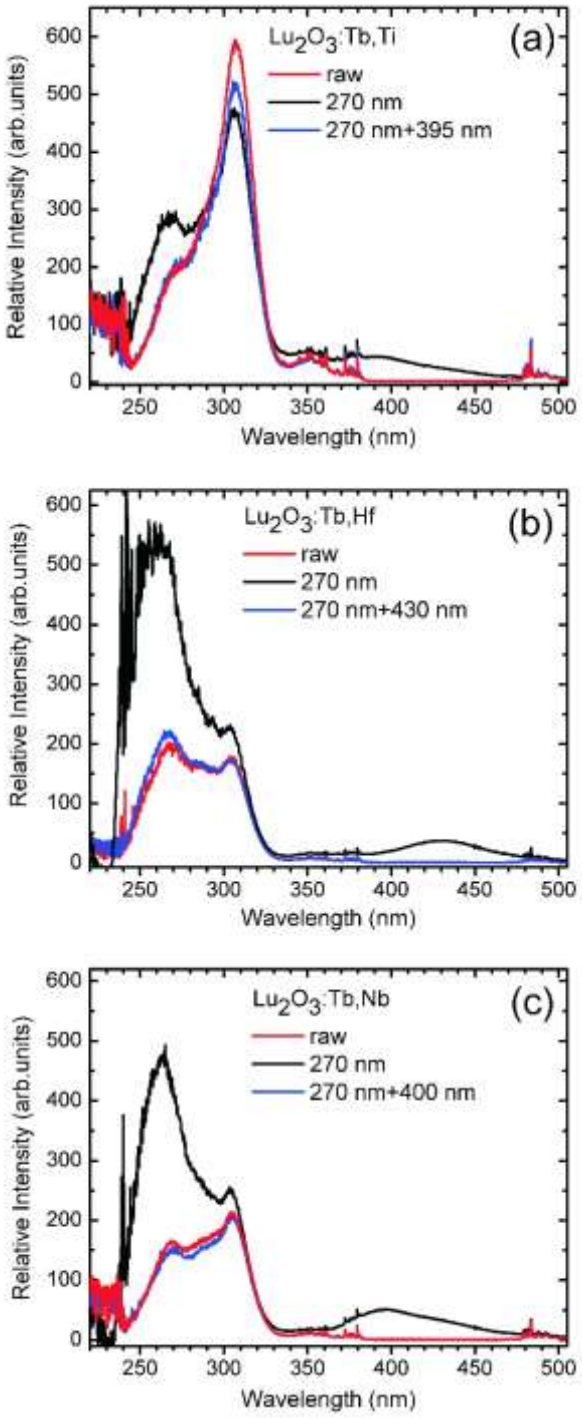

Fig. 10. Comparison of excitation spectra of the 542 nm luminescence of the Tb-series of specimens. The spectra were taken for an unirradiated (raw) specimen (red line), irradiated

with 270 nm radiation (black line) and the latter additionally irradiated into the induced excitation band around 400 nm for 20 minutes (blue line). In all cases the UV irradiation generated a broad band around 400 nm (ionizing radiation caused the same effects), while the subsequent irradiation into this component bleached it out completely.

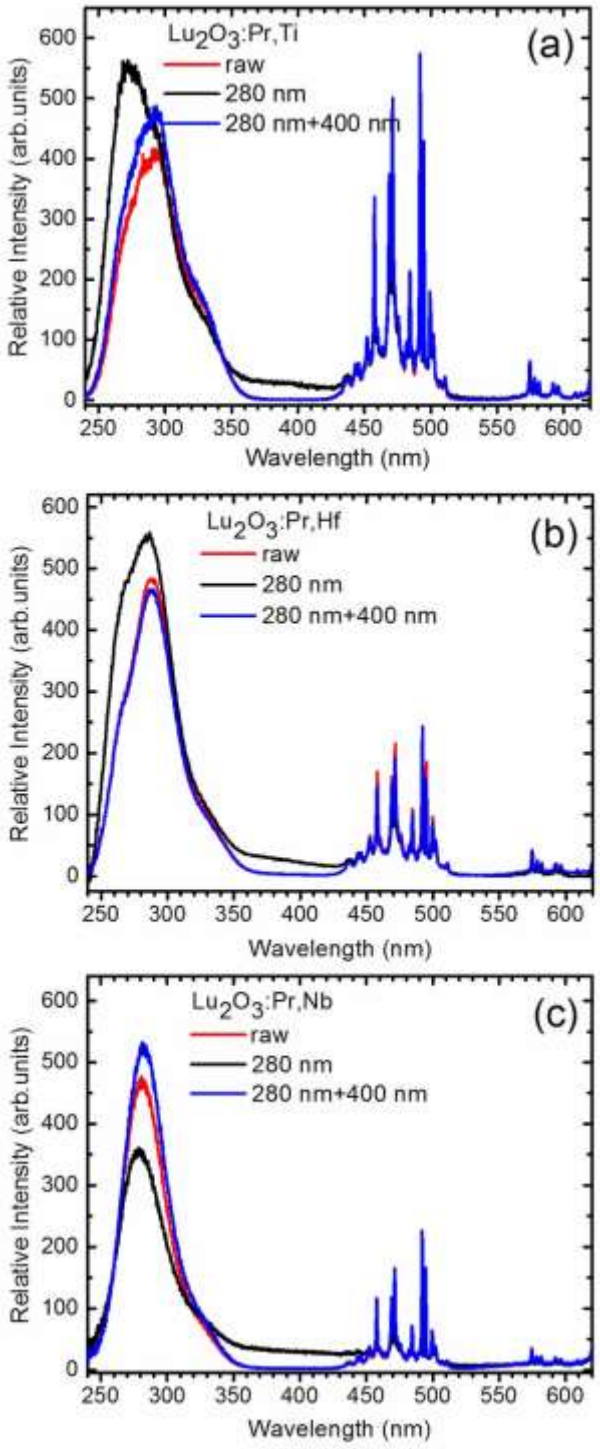

Fig. 11. Comparison of excitation spectra of the 631.5 nm luminescence of the Pr-series of specimens. The spectra were taken for an unirradiated (raw) specimen (red line), irradiated with 280

nm radiation (black line) and the latter additionally irradiated at 400 nm for 20 minutes (blue line). In all cases the UV irradiation generated a broad band around 400 nm (ionizing radiation caused the same effects), while the subsequent irradiation into this band bleached it out completely.

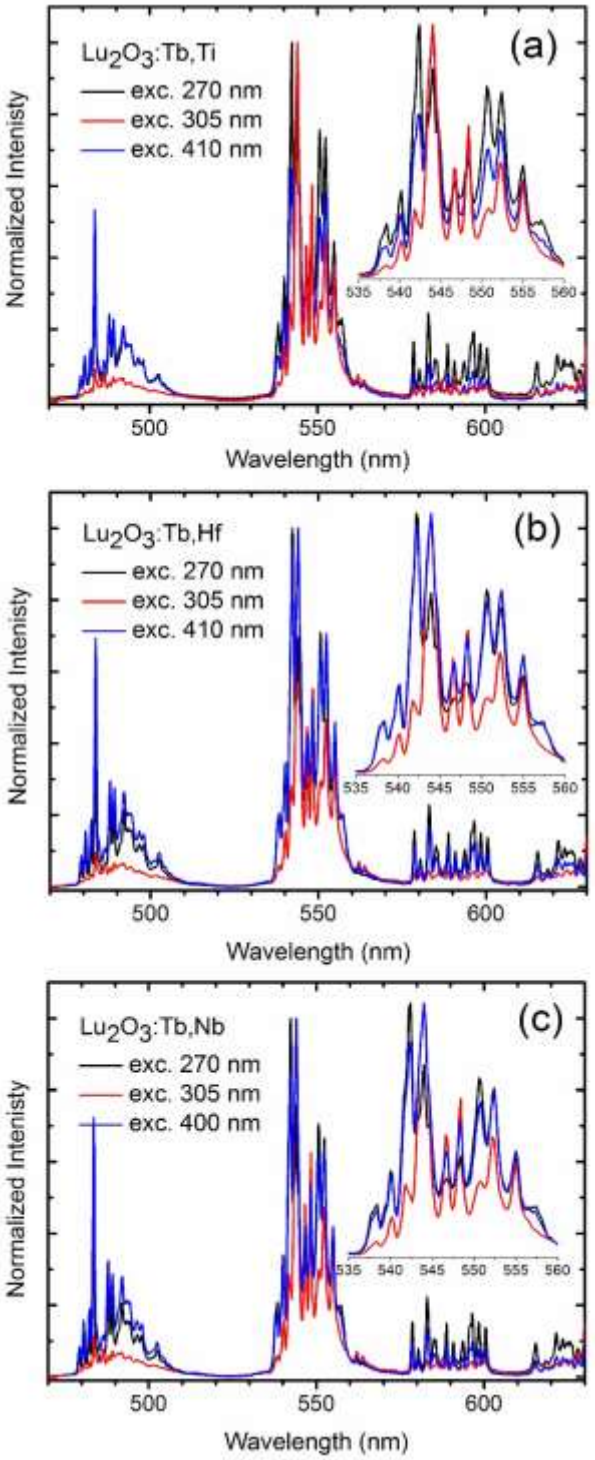

Fig. 12. Emission spectra of the three ceramics of the Tb-series upon 270 nm excitation (Tb in C_2 site), upon 305 nm (Tb in C_{3i} site) and under 410 nm optical stimulation into the band generated upon high energy photons. The OSL emissions are always composed of both the Tb(C_2) and Tb(C_{3i}) ions, proving

that the dopant participates in the energy storage independently on the symmetry site it occupies. Compare Fig. 13 for the Pr-series.

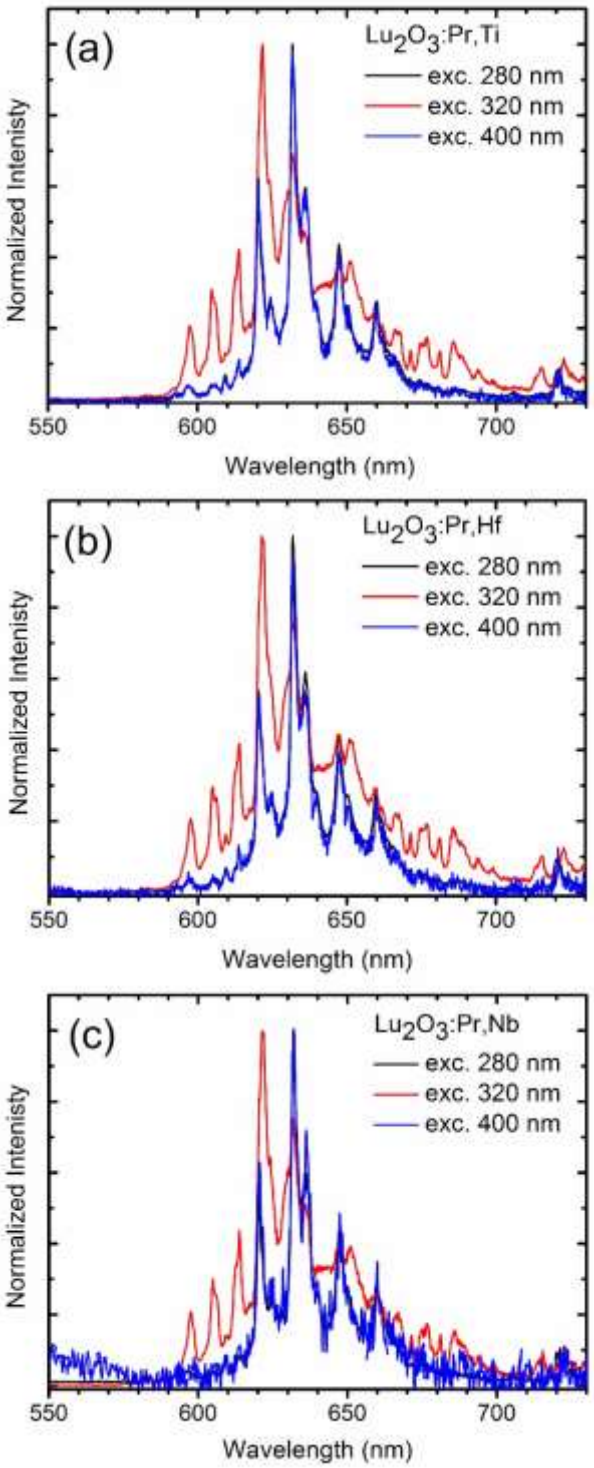

Fig. 13. Emission spectra of the three ceramics of the Pr-series upon 280 nm (Pr in C_2 site), and 320 nm (Pr in C_{3i} site) excitation and under 400 nm optical stimulation into the band generated upon high energy photons. The OSL emissions are always composed of only the Pr(C_2)-related components,

proving that only the Pr(C_2) dopant participates in energy storage. Compare with Fig. 12 for the Tb-series.

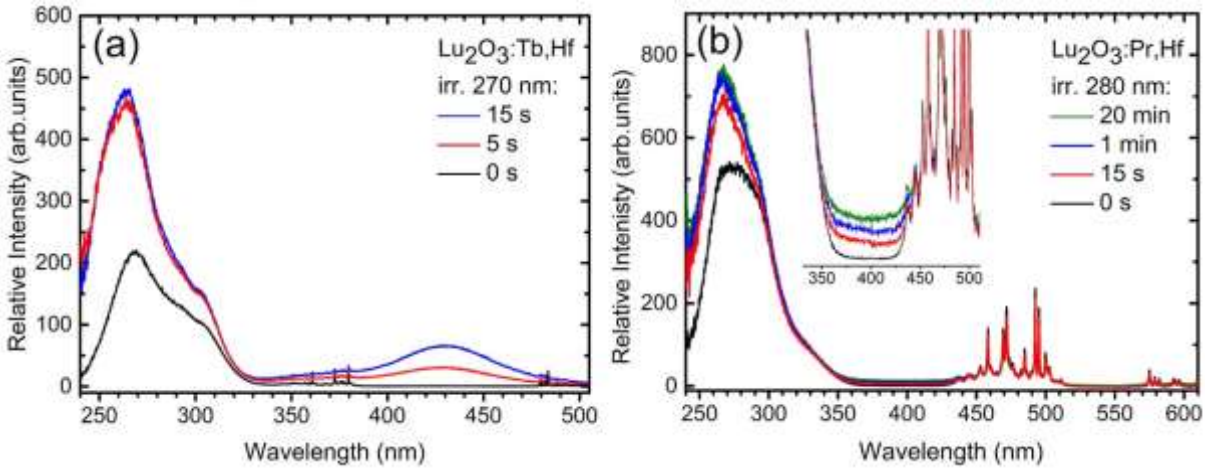

Fig. 14. Excitation spectra of Lu_2O_3:Tb,Hf (a) Lu_2O_3:Pr,Hf (b) recorded after different dose of UV radiation (270 or 280 nm).

References

[1] G. Blasse, B.C. Grabmaier, Luminescent Materials, Springer-Verlag, Berlin Heidelberg (1994).
[2] J. Botterman, P.F. Smet, Opt. Express 23 (2015) A868.
[3] H. Aizawa, T. Katsumata, J. Takahashi, K. Matsunaga, S. Komuro, T. Morikawa, E. Toba, Rev. Sci. Instrum. 74 (2003) 1344.
[4] W.M. Yen, S. Shionoya, H. Yamamoto, Phosphor Handbook, 2nd ed.; CRC Press: Boca Raton, FL, USA (2007).
[5] Z. Pan, Y.-Y. Lu, F. Liu, Nature Mat. 11 (2012) 58.
[6] W.M. Yen, M.J. Weber, Inorganic Phosphors: Compositions, Preparation and Optical Properties; CRC Press: Boca Raton, FL, USA (2004).
[7] W.M. Yen, S. Shionoya, H. Yamamoto, Phosphor Handbook, 2nd ed.; CRC Press: Boca Raton, FL, USA (2007).
[8] P.F. Smet, I. Moreels, Z. Hens, D. Poelman, Materials 3 (2010) 2834.
[9] E.N. Harvey, A history of luminescence from the earliest times until 1900. American Philosophical Society, Philadelphia (1957).
[10] M. Lastusaari, T. Laamanen, M. Malkamäki, K.O. Eskola, A. Kotlov, S. Carlson, E. Welter, H.F. Brito, M. Bettinelli, H. Jungner, J. Hölsä, Eur. J. Mineral. 24 (2012) 885.
[11] J.W. von Goethe, The Sorrows of Young Werther. Translated by T. Carlyle and R.D. Boylan. Ed. by Nathan Haskell Dole. Dover Publications, Inc. Mineola, New York (2002).
[12] J. Hölsä, The Electrochemical Society *Interface*, Winter (2009).
[13] K. Van den Eeckhout, D. Poelman, P. F. Smet, Materials 6 (2013) 2789.
[14] M. Bredol, J. Merikhi, C. Ronda, Ber. Bunsenges. Phys. Chem. 96 (1992) 1770.
[15] H. Lange, Luminescent Europium Activated Strontium Aluminate. US Patent 3,294,699, 1966.
[16] V. Abbruscato, J. Electrochem. Soc. 118 (1971) 930.
[17] G. Blasse, A. Bril, Philips Res. Rep. 23 (1968) 201.
[18] T. Matsuzawa, Y. Aoki, N. Takeuchi, Y. Murayama, J. Electrochem. Soc. 143 (1996) 2670.
[19] H. Takasaki, S. Tanabe, T. Hanada, J. Ceram. Soc. Jpn. 104 (1996) 322.

[20] Y. Lin, Z. Tang, Z. Zhang, C.W. Nan, Appl. Phys. Lett. 81 (2002) 996.
[21] Y. Lin, Z. Tang, Z. Zhang, X. Wang, J. Zhang, J. Mater. Sci. Lett. 20 (2001) 1505.
[22] Y. Lin, C.W. Nan, X. Zhou, J. Wu, H. Wang, D. Chen, S. Xu, Mater Chem. Phys. 82 (2003) 860.
[23] B. Liu, C. Shi, M. Yin, L. Dong, Z. Xiao, J. Alloy Compd 387 (2005) 65.
[24] W. Jia, H. Yuan, L. Lu, H. Liu, W.M. Yen, J. Lumin. 76-77 (1998) 424.
[25] D. Jia, W.M. Yen, J. Lumin. 101 (2003) 115.
[26] D. Jia, R.S. Meltzer, W.M. Yen, W. Jia, X. Wang, Appl. Phys. Lett. 80 (2002) 1535.
[27] D. Jia, W. Jia, D.R. Evans, W.M. Dennis, H. Liu, J. Zhu, W.M. Yen, J. Appl. Phys. 88 (2000) 3402.
[28] H.B. Yuan, W. Jia, S.A. Basun, L. Lu, R.S. Meltzer, W.M. Yen, J. Electrochem. Soc. 147 (2000) 3154.
[29] M. Saito, H. Hashimoto, Appl. Opt. 43 (2004) 3608.
[30] M. Saito, N. Adachi, H. Kondo, Opt. Express 15 (2007) 1621.
[31] H. Aizawa, T. Katsumata, K. Takahashi, S. Matsunaga, S. Komuro, T. Morikawa, E. Toba, Rev. Sci. Instrum. 74 (2003) 1344.
[32] T. Aitasalo, J. Hölsä, M. Jungner, J. Lastusaari, J. Niittykoski, J. Phys. Chem. B 110 (2006) 4589.
[33] J. Trojan-Piegza, J. Niittykoski, J. Hölsä, E. Zych, Chem. Mater. 20 (2008) 2252.
[34] J. Hölsä, M. Laamanen, M. Lastusaari, M. Malkamäki, P. Novák, J. Lumin. 129 (2009) 1606.
[35] M. Sonoda, M. Takano, J. Miyahara, H. Kato, Radiology 148 (1983) 833.
[36] S. Schweizer, phys. stat. sol. (a) 187 (2001) 335.
[37] P. Leblans, D. Vandenbroucke, P. Willems, Materials 4 (2011) 1034.
[38] P. Bilski, Radiat. Prot. Dosim. 100 (2002) 196.
[39] B. Obryk, H.J. Khoury, V.S. de Barros, P.L. Guzzo, P. Bilski, Radiat. Meas. 71 (2014) 25.
[40] P. Bilski, B. Marczewska, A. Twardak, E. Mandowska, A. Mandowski, Radiat. Meas. 71 (2014) 61.
[41] S.W.S. McKeever, M. Moscovitch, P.D. Townsend, Thermoluminescence Dosimetry Materials: Properties and Uses, Nuclear Technology Publishing, Ashford, UK (1995).
[42] G. Baldacchini, F. Bonfigli, F. Menchini, R.M. Montereali, Nucl. Instr. and Meth. in Phys. Res. B 191 (2002) 216.
[43] L. Oster, S. Druzhyna, Y.S. Horowitz, Nucl. Instr. and Meth. in Phys. Res. A 648 (2011) 261.
[44] M.S. Akselrod, V.S. Kortov, E.A. Gorelova, Radiat. Prot. Dosim. 47 (1993) 159.
[45] M. Budzanowski, P. Bilski, L. Bøtter-Jensen, A. Delgado, P. Olko, J.C. Sáez-Vergara, M.P.R. Waligórski, Radiat. Prot. Dosim. 66 (1996) 157.
[46] V. Kortov, Radiat. Meas. 42 (2007) 576.
[47] J. Azorín, R. Salvi, A. Moreno, Nucl. Instrum. Methods 175 (1980) 81.
[48] M. Prokić, Nucl. Instrum. Methods 175 (1980) 83.
[49] K.W. Crase, R.B. Gammage, Health Phys. 29 (1975) 739.
[50] E. Zych, Handbook of luminescence, display materials, and devices. Vol. 2. American Scientific Publishers (2003).
[51] Y. Zhydachevskii, A. Morgun, S. Dubinski, Y. Yu, M. Glowacki, S. Ubizskii, V. Chumak, M. Berkowski, A. Suchocki, Radiat. Meas. http://dx.doi.org/10.1016/j.radmeas.2015.12.001 (2015).
[52] Z. Spurný, Nucl. Instrum. Methods 175 (1980) 71.
[53] W.C Tsai, S.H. Jiang, Radiat. Meas. 46 (2011) 1595.
[54] S.S. Shinde, B.S. Dhabekar, B.C. Bhatt, Proceedings International Conference on Radiation Protection Measurements and Dosimetry: Current Practices and Future Trends, Mumbai, February 20 (2001).
[55] A.J.J. Bos, P. Dorenbos, A. Bessiere, B. Viana, Radiat. Meas. 43 (2008) 222.
[56] A.J.J. Bos, P. Dorenbos, A. Bessiere, A. Lecointre, M. Bedu, M. Bettinelli, F. Piccinelli, Radiat. Meas. 46 (2011) 1410.
[57] A. Lecointre, A. Bessiere, A.J.J. Bos, P. Dorenbos, B. Viana, S. Jacquart, The J. Phys. Chem. C 115 (2011) 4217.
[58] A. Dobrowolska, E.C. Karsu, A.J.J. Bos, P. Dorenbos, J. Lumin. 160 (2015) 321.
[59] M. Lastusaari, A.J.J. Bos, P. Dorenbos, T. Laamanen, M. Malkamaki, L.C.V. Rodrigues, J. Hölsä, J Therm Anal Calorim DOI 10.1007/s10973-015-4571-7 (2015).

[60] Y. Wang, L. Wang, J. Appl. Phys. 101 (2007) 053108.
[61] K. Van den Eeckhout, P.F. Smet, D. Poelman, Materials 3 (2010) 2536.
[62] C.W. Thiel, H. Cruguel, H. Wu, Y. Sun, G.J. Lapeyre, R.L. Cone, R.W. Equall, R.M. Macfarlane, Phys. Rev. B 64 (2001) 085107.
[63] C.W. Thiel, R.L. Cone, J. Lumin. 131 (2011) 386.
[64] P. Dorenbos, J. Phys. Condens. Matter 15 (2003) 8417.
[65] P. Dorenbos, J. Lumin. 111 (2005) 89.
[66] P. Dorenbos, J. Alloy Compd 488 (2009) 568.
[67] E.G. Rogers, P. Dorenbos, ECS J. Solid State Sci. Technol. 3 (2014) R173.
[68] E.G. Rogers, P. Dorenbos, J. Lumin. 153 (2014) 40.
[69] J. Pejchal, Y. Fujimoto, V. Chani, F. Moretti, T. Yanagida, M. Nikl, Y. Yokota, A. Beitlerova, A. Vedda, A. Yoshikawa, J. Cryst. Growth 318 (2011) 828.
[70] J. Pejchal, Y. Fujimoto, V. Chani, T. Yanagida, Y. Yokota, A. Yoshikawa, M. Nikl, A. Beitlerova, J. Cryst. Growth 360 (2012) 127.
[71] Y. Ji, D. Jiang, J. Shi, J. Mater. Res. 20 (2005) 567.
[72] S.W.S. McKeever, Thermoluminescence of solids, Cambridge University Press, Cambridge (1985).
[73] R. Chen, S.W.S. McKeever, Theory of Thermoluminescence and Related Phenomena, World Scientific Publishing Co. Pte. Ltd. (1997).
[74] S.W.S. McKeever, R. Chen, Radiat. Meas. 27 (1997) 625.
[75] R. Visocekas, Radiat. Prot. Dosim. 100 (2002) 45.
[76] R. Visocekas, T. Ceva, C. Marti, F. Lefaucheux, M.C. Robert, Phys. Stat. Sol (a) 35 (1976) 315.
[77] A. Dobrowolska, A.J.J. Bos, P. Dorenbos, J. Phys. D: Appl. Phys. 47 (2014) 335301.
[78] J. Ueda, K. Kuroishi, S. Tanabe, Proc. of SPIE 8987 (2014) 89870L-1.
[79] J. Ueda, P. Dorenbos, A.J.J. Bos, K. Kuroishi, S. Tanabe, J. Mater. Chem. C 3 (2015) 5642.
[80] K. Kamada, T. Endo, K. Tsutumi, T. Yanagida, Y. Fujimoto, A. Fukabori, A. Yoshikawa, J. Pejchal, M. Nikl, Cryst. Growth Des. 11 (2011) 4484.
[81] N. Cherepy, J. Kuntz, Z. Seeley, S. Fisher, O. Drury, B. Sturm, T. Hurst, J. Roberts, S. Payne, SPIE Newsroom, 10.1117/2.1201009.003196 (2010).
[82] M. Kucera, M. Hanus, Z. Onderisinova, P. Prusa, A. Beitlerova, M. Nikl. IEEE Transactions on Nuclear Science 61 (2014) 282.
[83] M. Fasoli, A. Vedda, M. Nikl, C. Jiang, B.P. Ubeuraga, D.A. Andersson, K.J. McClellan, C.R. Stanek, Phys. Rev. B 84 (2011) 081102(R).
[84] D. Poelman, O.Q. De Clercq, P.F. Smet, K. Braeckmans, ECS Meeting Abstracts MA2015-02 1593.
[85] Y. Zorenko, A. Voloshynovskii, V. Vistovsky, M. Grinberg, A. Kornylo, T. Łukasiewicz, M. Świrkowicz, phys. stat. sol. (b) 244 (2007) 3271.
[86] J.D. Tilley, Defects in Solids, John Wiley & Sons, Inc. 2008.
[87] E. Zych, J. Trojan-Piegza, D. Hreniak, and W. Stręk, J. Appl. Phys. 94 (2003) 1318.
[88] J. Trojan-Piegza, E. Zych, J. Hölsä, J. Niittykoski, Phys. Chem. C 113 (2009) 20493.
[89] J. Trojan-Piegza, J. Niittykoski, J. Hölsä, E. Zych, Chem. Mater. 20 (2008) 2252.
[90] D. Kulesza, A. Wiatrowska, J. Trojan-Piegza, T. Felbeck, R. Geduhn, P. Motzek, E. Zych, U. Kynast, J. Lumin. 133 (2013) 51.
[91] S. Chen, Y. Yang, G. Zhou, Y. Wu, P. Liu, F. Zhang, S. Wang, J. Trojan-Piegza, E. Zych, Opt. Mater. 35 (2012) 240.
[92] S. Erdei, L. Kovksb, M. Martini, F. Meinardi, F.W. Ainger, W.B. White, J. Lumin. 68 (1996) 27.
[93] E. Zych, D. Kulesza, J. Zeler, J. Cybińska, K. Fiaczyk, A. Wiatrowska, ECS J. Solid State Sci. Technol. 5 (2016) R3078.
[94] M. Pechini, Method of preparing lead and alkaline earth titanates and niobates and coating method using the same to form a capacitor. US Patent No. 3330697 A, 1967.
[95] A. Wiatrowska, E. Zych, P. Bolek, X-ray memory as well as its use. Patent WO 2014/200372 A1, PCT/PL2014/050001, 2014.
[96] D. Kulesza, J. Trojan-Piegza, E. Zych, Radiat. Meas. 45 (2010) 490.

[97] A. Wiatrowska, E. Zych, Materials 7 (2014) 157.
[98] A. Wiatrowska, E. Zych, J. Phys. Chem. C 117 (2013) 11449.
[99] D. Kulesza, E. Zych, J. Phys. Chem. C. 117 (2013) 26921.
[100] A.J.J. Bos, D. Kulesza, E. Zych, 9th International Conference on Luminescent Detectors and Transformers of Ionizing Radiation (Lumdetr 2015) – Tartu, Estonia in September, 20 – 25, 2015.
[101] C. de Mello Donegá, PhD Thesis: Vibronic spectroscopy of Pr^{3+} in solids, 1994.
[102] J.L. Pascual, Z. Barandiarán, L. Seijo, Theor. Chem. Acc. 129 (2011) 545.
[103] A.M. Srivastava, C. Renero-Lecuna, D. Santamaría-Pérez, F. Rodríguez, R. Valiente, J. Lumin. 146 (2014) 27.
[104] R.T. Wegh, A. Meijerink, Phys. Rev. B 60 (1999) 10820.
[105] L. Van Pieterson, M.F. Reid, G.W, Burdick, A. Meijerink, Phys. Rev. B 65 (2002) 045114.
[106] E. Zych, J. Trojan-Piegza, J. Lumin. 122-123 (2007) 335.